Performance Test of Pulse Tube Cooler with Integrated Circulator

J.R. Maddocks, P. Maddocks, M. Fay,
B.P.M. Helvensteijn, A. Kashani

Atlas Scientific
San Jose, CA 95120

ABSTRACT

To address the need for remote and broad area cooling using regenerative cryocoolers, Atlas Scientific is developing a lightweight, continuous-flow Integrated Circulator (IC) for installation on Pulse Tube Cryocoolers (PTCs). The basis of the IC is a rectifier that converts the oscillating flow of a regenerative cryocooler into a steady flow of cold gas that can readily be distributed over distances of several meters to multiple or broad area thermal loads. The Integrated Circulator has advantages over competing technologies, such as the use of a secondary mechanical or capillary pump dedicated to circulating cryogens through a cold heat exchanger conductively coupled to the coldhead of the cryocooler, in that it eliminates the pump, its potential reliability problems, its parasitic power consumption, and the additional temperature rise introduced by the presence of the conductively coupled heat exchanger at the PTC coldhead. Here, we report on PTC performance measurements made both with and without the presence of an Integrated Circulator. Such measurements are necessary in order to make quantitative comparisons of the IC to competing technologies. The results indicate that the IC is indeed a viable alternative.

INTRODUCTION

Interest in thermal management of space-based, as well as ground-based cryogenic systems for aerospace applications, has increased over the past several years. Specifically, interest has developed in zero boil-off technologies, such as improved multi-layer insulations and broad area cooling scenarios that require cryogenic circulators, as well as, remote cooling of multiple sensors and in situ liquefaction of cryogenic propellants. However, thermal control strategies at low temperature are often limited by the lack of readily available hardware designed specifically for and qualified for cryogenic use. To address the need for remote and broad area cooling using regenerative cryocoolers, Atlas Scientific is developing a lightweight, continuous-flow Integrated Circulator (IC) for installation on Pulse Tube Cryocoolers (PTCs) and Stirling cryocoolers.

The most well-known cooling loops are the Loop Heat Pipe (LHP),[1] its close cousin the Capillary Pumped Loop (CPL) and the Mechanically Pumped Loop (MPL) with either a cryogenic pump[2] or an ambient pump.[3] Each configuration envisions a cooling loop that is

Cryocoolers 16, edited by S.D. Miller and R.G. Ross, Jr.

dedicated to circulating cold fluid through a heat exchanger thermally connected to the coldhead of a cryocooler.

A lesser-known alternative, but one that has gained attention recently, is the Integrated Circulator (IC). The IC is made possible by integrating a rectifying interface into the cold heat exchanger of a regenerative cryocooler. The interface withdraws and rectifies a small portion of the oscillating flow in the coldhead, converting it into a steady flow of refrigerant gas that is easily distributed throughout the volume of a dewar or over the surface of a shield, mirror, sunshade, or other large device without requiring a separate circulating pump. The IC avoids a number of specific disadvantages associated with other options. For example, because the IC is directly integrated with the cryocooler, fluid flow in the cooling loop is obtained from and returns to the gas volume of the coldhead. Therefore, no external heat exchanger at the coldhead is required. Also, there is no parasitic power consumption (as with a mechanically driven circulator) nor is there orientation dependence (as with the capillary pumped loop).

The IC provides a substantial pressure difference to drive the circulating fluid flow, nominally equal to the peak-to-peak pressure swing that occurs in the cryocooler. As a consequence, the flow can be forced through long lengths of small diameter tubing. This arrangement provides for a large heat transfer coefficient, facilitates cooling across flexible joints and gimbals and allows a substantial pressure drop to be incurred across a flow control valve, thereby enabling tight temperature control via flow modulation. To address potential contamination issues associated with spacecraft integration, getters may be incorporated into the buffer volumes.

In the following sections we present a lumped parameter thermal model followed by PTC performance measurements made both with and without the presence of an Integrated Circulator. Comparison of model calculations and performance measurements indicates that the simple model captures the essentials of IC performance.

THERMAL MODEL

We developed a thermal model of the Integrated Circulator, based on the schematic representation shown in Fig.1, to facilitate understanding of its behavior and make quantitative comparisons between the IC and other remote cooling options. To accomplish this we write a set of equations that describe the thermodynamic state of the fluid at each of eight locations around the loop: the inlet and outlet of each check valve, the interior of each buffer volume and the inlet and outlet of the remote load. In this way we are able to account for pressure drop across the check valves and flow loop, parasitic heat leaks to the buffer volumes and flow loop and a remote heat load in the center of the flow loop.

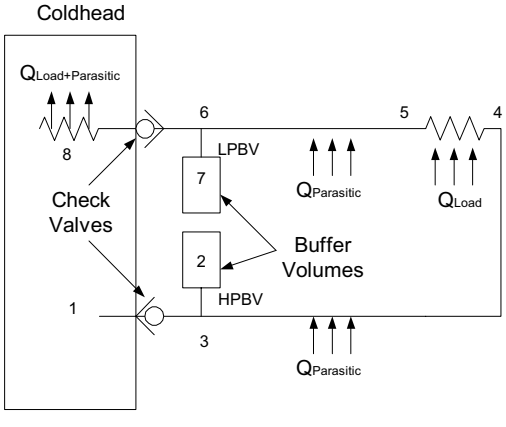

Figure 1. Schematic representation of Integrated Circulator concept. The numerals 1 through 8 indicate the locations to which the thermodynamic *States* 1 through 8, referred to in the text, correspond.

We start by taking *state* 1 to be the gas in the coldhead before it enters the loop, so it is at the high pressure and the coldhead temperature (T_1). This temperature is related to the heat load on the cryocooler by the measured load line

$$\dot{Q}_{load} = m\left(T_1 - T_0\right), \tag{1}$$

where m is the slope of the heat load-line, and T_0 is the no-load temperature.

The high pressure check valve opens when the coldhead pressure rises above that in the high-pressure buffer volume (HPBV). There is a small pressure drop associated with the check valve so that, as the gas enters the HPBV and reaches *State* 2, it is at a slightly lower pressure than *State* 1. This expansion is assumed to be isenthalpic. The pressure at 2 is given by

$$P_2 = P_1 - \Delta P_{cv} \tag{2}$$

The HPBV has a small parasitic heat leak, which is assumed to be a simple number of watts. This heat leak increases the enthalpy of the gas from the inlet to the outlet of the HPBV. The enthalpy at *State* 3, the outlet of the HPBV, is given by

$$\dot{Q}_{para,HPBV} = \dot{m} \cdot \left(h_3 - h_2\right) \tag{3}$$

and it is further assumed that $P_3 = P_2$.

From the outlet of the buffer, the gas enters the cooling loop. The pressure difference across the loop is fixed by the pressure difference between the buffer volumes. A resistance is required in the loop to limit the mass flow rate. The value of the required resistance is an output of the model, calculated as

$$R = \frac{\Delta P}{\dot{V}} = \frac{\rho \Delta P}{\dot{m}} \tag{4}$$

From knowledge of the resistance, the required loop geometry can be determined. Because we used a metering valve in our experiment, the model assumes that the entire pressure drop occurs across this valve, which is located after the load.

In addition to pressure losses, there is parasitic heat leak on the loop and valve. The parasitic heat loss is a number of watts, (measured experimentally) which increases the enthalpy of the gas from *State* 3 to 4, the entrance to the load heat exchanger.

$$\dot{Q}_{para1} = \dot{m} \cdot \left(h_4 - h_3\right) \tag{5}$$

The heat load is applied between *State* 4 and 5, and the pressure at 5 is assumed to be the same as that of *State* 2, so that

$$\dot{Q}_{load} = \dot{m} \cdot \left(h_5 - h_4\right) \tag{6}$$

The return segment of the loop, between the load and low pressure buffer volume (LPBV) accounts for the total pressure drop and again has a parasitic heat load associated with it. It is assumed the valve is isenthalpic so the enthalpy change from the heat leak is the only change in enthalpy between *States* 5 and 6. The parasitic heat load creates a rise in enthalpy,

$$\dot{Q}_{para2} = \dot{m} \cdot \left(h_6 - h_5\right). \tag{7}$$

Since the total change in pressure around the loop is assumed to take place in the valve, the pressure at *State* 6 is at the same pressure as the LPBV.

From *State* 6 at the inlet of the LPBV, there is another parasitic heat load just as with the HPBV given by

$$\dot{Q}_{para,LPBV} = \dot{m} \cdot \left(h_7 - h_6\right) \tag{8}$$

States 6 and 7 in the LPBV have a pressure that is slightly higher than the minimum in the coldhead. The difference is a result of the small pressure drop associated with the check valve, which again is assumed isenthalpic.

$$P_6 = P_7 = \left(P_{mean} - P_{pt}\right) - \Delta P_{cv} \tag{9}$$

Finally, the cryocooler must pressurize the return gas to *State* 8 (high pressure, high temperature), then cool it back to the conditions of *State* 1 (high pressure, low temperature). The work to re-pressurize the gas is given by

$$\dot{W}_{pump,isen} = \dot{m} \cdot R_{He} \cdot T_7 \left(\frac{\gamma}{\gamma - 1} \right) \left(\left(\frac{P_7}{P_8} \right)^{\left(\gamma - 1 \right) / \gamma} - 1 \right) \tag{10}$$

in which the work is approximated as being isentropic, since a single pulse tube cycle takes very little time. The temperature following compression is given by

$$\frac{T_8}{T_7} = \left(\frac{P_8}{P_7} \right)^{\left(\gamma - 1 \right) / \gamma} \tag{11}$$

and the cooling power required to cool the gas from T_8 back to T_1 is given by the difference in enthalpies between the high-pressure, high-temperature, *State* 8, and the initial, high-pressure, low-temperature, *State* 1.

$$\dot{Q}_{pt} = \dot{m} \cdot \left(h_8 - h_1 \right) \tag{12}$$

From these 12 equations, the thermodynamic state of the fluid at each of the eight locations can be determined, given values for the parasitic heat loads, the buffer pressures (assuming they are reasonably constant) and the load line of the cryocooler.

EXPERIMENTAL PROCEDURE AND TEST RESULTS

To accomplish the performance measurements, we modified an existing pulse tube design. Because the PTC without IC performs well, the IC flange was carefully designed to leave the internal geometry of the PTC unchanged. A photograph of the assembled pulse tube with IC flange is shown in Fig. 2. Flow to the IC is extracted from the cold heat exchanger and returned to the cold heat exchanger in parallel with the main flow out of the regenerator and into the pulse tube.

We first measured a baseline heat load curve. The PTC was tested without the buffer volumes or flow loop attached. The IC flange was installed and so represented the presence of a slightly larger parasitic heat load than the original design. During this run, installing a Kapton gasket between the cold heat exchanger and the check-valve flange to cover the IC supply holes blocked off the internal volume of the IC flange. The only additional dead volume, then, was that associated with the supply holes in the CHX, which was considered negligible.

Figure 2. Pulse tube cold head, with Integrated Circulator installed, ready for testing

Two thermocouples and a platinum resistance thermometer (PRT) were mounted on the IC flange above the cold heat exchanger. A heater was mounted on the PTC cold heat exchanger and a thermocouple on the hot heat exchanger to monitor operating temperature. Ten layers of MLI were wrapped around the pulse tube, IC flange and regenerator. An additional 10 layers were laid atop the bottom regenerator flange.

We operated the cooler at 60 Hz, at which frequency it reached a no-load temperature of 45 K, compared to a previous best of 41 K reached while operating at 64 Hz. The difference is likely due at least in part to the additional parasitic load associated with the Integrated Circulator flange. Differences in operating frequency, MLI design and vacuum pressure may also account for some of the discrepancy.

Several heat loads between zero and 13 watts were applied to the cold heat exchanger to determine the heat load curve. The data, shown graphically in Fig. 3, indicate that the load line is linear over this range of heat inputs with a slope of 0.228 W/K. This is to be compared with 0.226 W/K measured while operating at 64 Hz without an IC flange.

Following measurement of the baseline heat load curve, we installed the buffer volumes, each with a thermocouple mounted to its exterior surface. The internal dead volume of the IC flange was still blocked and no flow loop was installed. MLI, ten layers, was added to the buffers. In this configuration, we measured a no-load temperature of 53.4 K and determined the parasitic heat load associated with the buffer volumes by use of the baseline heat load curve to be 2 W. This can be reduced by doing a more effective job of designing and installing the MLI. In most cases, MLI has an effective thermal conductivity that is dominated by conduction through the contact between layers. This is the case when the number of layers is large and the vacuum is below 1 x 10^{-4} torr. Increasing the number of layers by a factor of two will cut the heat leak approximately in half as long as the layer density (layers/inch) remains the same.

In a third configuration, the internal volume of the IC flange was opened up, but no flow allowed through the loop. This gives a measure of the effect of increasing the dead volume at the cold end of the regenerator. The measured heat load curve is shown in Fig. 4. The slope of the curve is slightly less than the baseline, perhaps indicating that the losses have a small dependence on temperature. The increase in no-load temperature from 53.4 to 61.8 corresponds to an additional heat load of approximately 2 watts.

However, in this configuration we observed that there appeared to be some leakage flow in the high pressure check valve. This is evident in the pressure trace shown in Fig. 5. Because there is no flow in the loop, the pressure loss on the high side is evidence for this. Leakage flow has the effect of adding dead volume to the cold head. Such volume can be estimated as a fraction of the buffer volume, where the fraction is given by the ratio of the pressure loss to the pulse tube pressure amplitude.

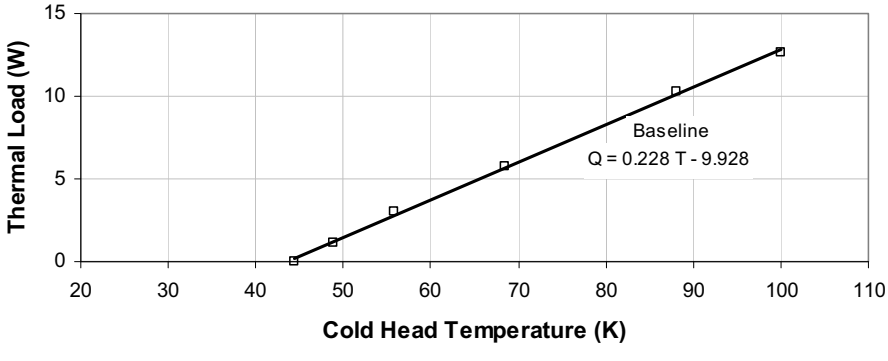

Figure 3. Heat load line for PTC with IC flange installed – no buffers or flow loop

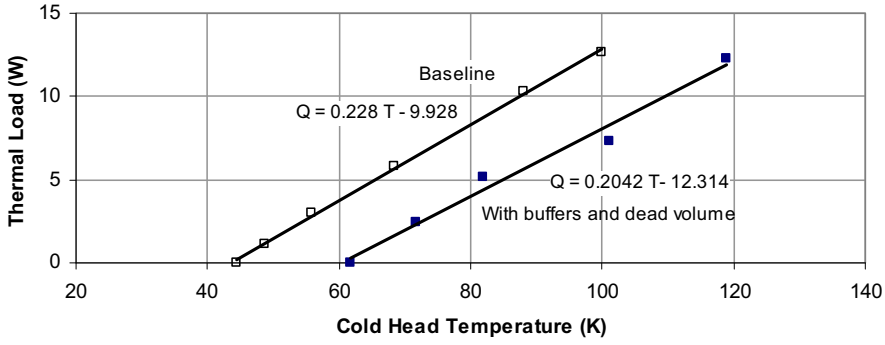

Figure 4. Comparison of heat load curves taken with buffers and dead volume installed to baseline.

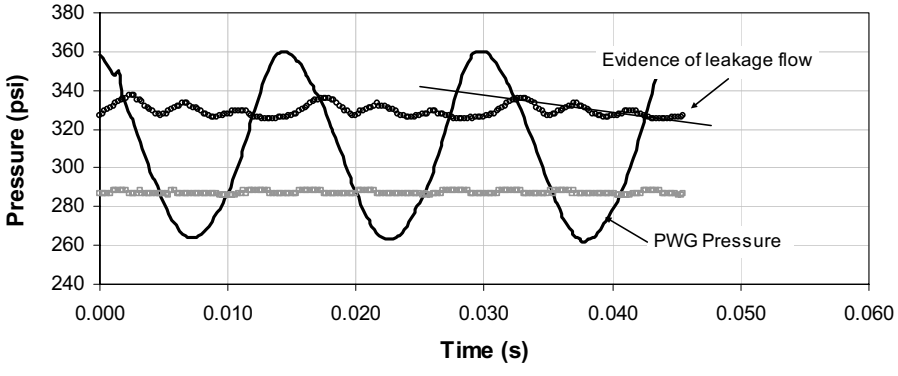

Figure 5. Pressure traces showing PWG together with high and low buffer pressures. Because there is no flow in the loop, the pressure loss on the high side is evidence of leakage flow.

We installed a new reed and repeated the test. The new no-load temperature was 56.2 K, a reduction in apparent heat load of 1.3 W. The resulting heat load curve is shown in Fig. 6.

Finally, a series of heat load curves at varying flow rates were measured. A flow loop with two valves, one shut-off and one metering, was installed between the buffer volumes. A heater was mounted on the flow loop midway between the buffers to simulate a thermal load. Each valve was instrumented with a thermocouple so that the steady state could be identified. Finally, two PRTs were mounted in the gas stream of the flow loop, one immediately upstream of the loop heater and one immediately downstream. These provided a measure of the average mass flow rate, as well as, a measure of the load temperature.

A load curve with the loop installed, but without flow is shown in Fig.7. These data give an indication of the parasitic heat load associated with the valves and the loop. The no-load temperature of 67.5 K indicates a heat load associated with the loop and valves of 2.7 watts. The curve serves as an adjusted baseline for heat load measurements taken with heat applied to the loop at various flow rates. The various parasitic heat losses are tabulated in Table 1.

Table 1. Tabulation of measured parasitic heat losses.

Loss Mechanism	*Loss in watts*
Heat load on buffers	2
Dead volume (leaky valve fixed)	0.7
Leaky valve	1.3
Cooling loop	2.7

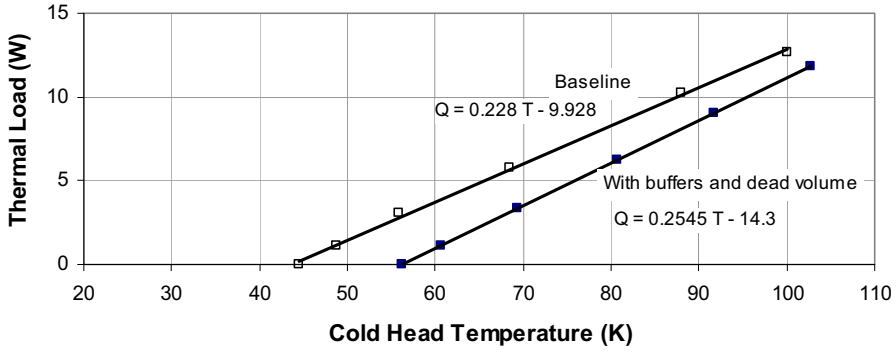

Figure 6. Heat load curve with buffers installed and additional dead volume of IC at cold end. Data are from test conducted after the leaking reed was replaced.

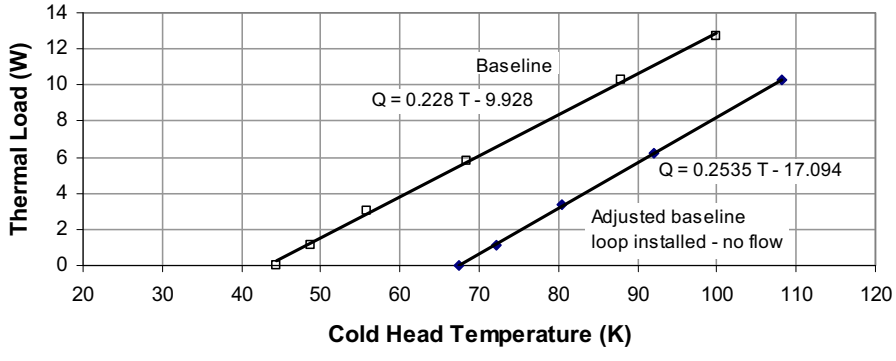

Figure 7. Adjusted baseline load curve – buffer volumes and cooling loop installed but no flow.

Following establishment of the adjusted baseline load curve, a series of heat load curves for various valve settings were measured. The results for three of these settings are shown in Fig. 8. The heat loads were applied at the remote load. Temperatures are the average of inlet and outlet. Note that a remote heat load of 6 watts, for example, results in three different temperatures for the three different valve settings. To understand the meaning of this result, the load temperature as a function of mass flow rate for fixed heat inputs is plotted in Fig. 9.

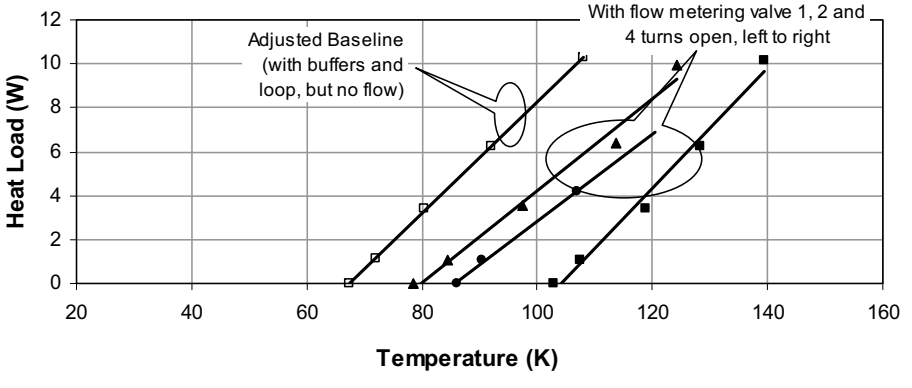

Figure 8. Comparison of heat lift capability as function of increasing flow rate in the cooling loop

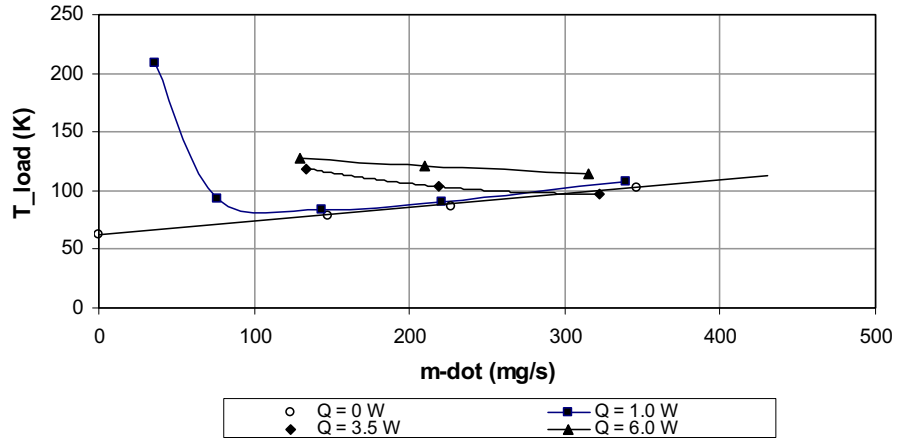

Figure 9. Graph of the load temperature as a function of mass flow rate. Note that the no-load data serves as a lower bound on the load temperature.

There we see that at very low flow rates the average temperature rises because the temperature from inlet to outlet of the remote load rises dramatically, even for relatively small heat inputs. As the loop flow rate increases this temperature rise is reduced. There is a limit, though, to how much one can increase the flow rate, since doing so reduces PTC performance, resulting in an overall rise in the average system temperature. The two competing effects result in the presence of an optimum flow rate for a given heat load and temperature. For reference, the RMS mass flow rate at the pressure wave generator is approximately 3.4 g/s, so that the flow rates in Fig. 9 are in the range of 1.5 to 12.5 percent of flow into the regenerator.

COMPARISON OF MODEL CALCULATIONS AND TEST RESULTS

Results of the modeling effort are presented in Fig. 10, where the load temperature is plotted versus the mass flow rate. The lines are calculated. The dotted line predicts the coldhead temperature for the case of flow in the loop, but without heat added. The open squares are data measured at various flow rates for the same case. The solid line predicts the load temperature for a heat input of 1 watt at the remote load. The solid squares are measured data for the case of 1 watt added at the remote load. In both cases this simple model agrees well with experiment. In making the calculations, measured values of parasitic heat load on the buffer volumes and cooling loop from Table 1 were used. The presence of an optimal mass flow rate, as observed experimentally, is nicely captured by this simple model.

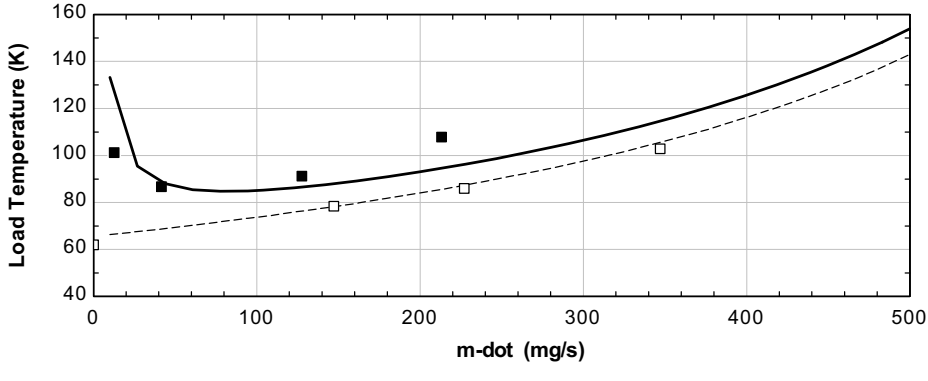

Figure 10. Comparison of modeling results to data from test measurements.

SUMMARY

We have measured the effect of an Integrated Circulator on the performance of a pulse tube cryocooler. Such measurements are necessary in order to make quantitative comparisons of the IC to the CPL, LHP and mechanically pumped loops. The primary effect, for flows on the order of 10 percent of the flow into the PTC cold heat exchanger, is that of a simple heat load, which leaves the slope of the baseline load curve essentially unchanged. In addition, we find that for a given temperature and heat load there is an optimum mass flow rate.

ACKNOWLEDGMENT

The authors wish to thank NASA Goddard Spaceflight Center for supporting this project under SBIR Grant # NNX09CD51P

REFERENCES

1. T.T. Hoang, T.A. O'Connell, J. Ku, C.D. Butler, T.D. Swanson, "Large Area Cooling for Far Infrared Telescopes," *Cryogenic Optical Systems and Instruments X*, Proceedings of SPIE Vol. 5172 (2003).
2. A. Hedayat, L. J. Hastings, C. Bryant, and D. W. Plachta, "Large Scale Demonstration of Liquid Hydrogen Storage with Zero Boil-off," *Adv. in Cryogenic Engineering*, Vol. 47B, Amer. Institute of Physics, Melville, NY (2002), pp. 1276-1283.
3. M. Michaelian, T. Nguyen, M. Petach, J. Raab, "Remote Cooling with the HEC Cooler," *Cryocoolers 15*, ICC Press, Boulder, CO (2009), pp. 541-544.